

Low-frequency noise sources in as-prepared and aged GaN-based light-emitting diodes

Citation for published version (APA):

Bychikhin, S., Pogany, D., Vandamme, L. K. J., Meneghesso, G., & Zanoni, E. (2005). Low-frequency noise sources in as-prepared and aged GaN-based light-emitting diodes. *Journal of Applied Physics*, 97(12), 123714-1/7. Article 123714. <https://doi.org/10.1063/1.1942628>

DOI:

[10.1063/1.1942628](https://doi.org/10.1063/1.1942628)

Document status and date:

Published: 01/01/2005

Document Version:

Publisher's PDF, also known as Version of Record (includes final page, issue and volume numbers)

Please check the document version of this publication:

- A submitted manuscript is the version of the article upon submission and before peer-review. There can be important differences between the submitted version and the official published version of record. People interested in the research are advised to contact the author for the final version of the publication, or visit the DOI to the publisher's website.
- The final author version and the galley proof are versions of the publication after peer review.
- The final published version features the final layout of the paper including the volume, issue and page numbers.

[Link to publication](#)

General rights

Copyright and moral rights for the publications made accessible in the public portal are retained by the authors and/or other copyright owners and it is a condition of accessing publications that users recognise and abide by the legal requirements associated with these rights.

- Users may download and print one copy of any publication from the public portal for the purpose of private study or research.
- You may not further distribute the material or use it for any profit-making activity or commercial gain
- You may freely distribute the URL identifying the publication in the public portal.

If the publication is distributed under the terms of Article 25fa of the Dutch Copyright Act, indicated by the "Taverne" license above, please follow below link for the End User Agreement:

www.tue.nl/taverne

Take down policy

If you believe that this document breaches copyright please contact us at:

openaccess@tue.nl

providing details and we will investigate your claim.

Low-frequency noise sources in as-prepared and aged GaN-based light-emitting diodes

S. Bychikhin and D. Pogany^{a)}

Institute for Solid State Electronics, Vienna University of Technology, A-1040 Vienna, Austria

L. K. J. Vandamme

Department of Electrical Engineering, Eindhoven University of Technology, 5600MB Eindhoven, The Netherlands

G. Meneghesso and E. Zanoni

Department of Information Engineering, University of Padova, 35131 Padova, Italy

(Received 15 December 2004; accepted 4 May 2005; published online 29 June 2005)

The low-frequency noise sources are investigated in as-prepared and aged GaN light-emitting diodes (LEDs). Accelerated aging is performed by thermal (300 h at 240 °C) and electrical forward-bias stressing (20 and 50 mA for 2500 h). At low currents $I < I_{\text{RTS}}$, where I_{RTS} is a critical current, the low-frequency noise is dominated by random telegraph signal (RTS) noise on top of the $1/f$ noise. An explanation is given for the giant relative current jumps $\Delta I/I \approx 50\%$ and an expression for I_{RTS} is derived. The RTS noise in our devices is a less-sensitive diagnostic tool for studying the results of accelerated aging. Two components of the $1/f$ noise were observed: one is related to the quantum-well junction and the other is due to series resistance noise. The two $1/f$ spectra have different current dependences. It was found that the junction $1/f$ noise is not significantly affected by aging. However, a strong increase in series resistance noise, by a factor of 60–800 compared to unstressed devices, is observed after strong electrical and thermal aging. This high increase goes hand in hand with a relatively small increase in the value of the series resistance (13%–90%). This makes $1/f$ noise a very sensitive reliability indicator for GaN LEDs after accelerated aging. We discuss the physical origin of LED degradation. © 2005 American Institute of Physics.
[DOI: 10.1063/1.1942628]

I. INTRODUCTION

At present light-emitting diodes (LEDs) are substituting more and more for conventional light sources in daily life. LEDs based on GaN offer ultrabrightness (from visible blue up to ultraviolet region) and a high electrical efficiency.^{1–3} The growing market of GaN LEDs requires higher reliability and longer lifetime of these devices.⁴ Therefore, finding the physical origin of the degradation mechanisms and having sensitive reliability indicators are important. The degradation modes and stress-induced defects in GaN LEDs due to thermal, direct current (dc), and pulsed electrical stress have been investigated recently by dc current–voltage (IV) characterization, light-emission mapping, capacitance dispersion, and deep-level transient spectroscopy.^{5–7} The light-emission decrease with aging has been correlated with an increase in contact resistance, leakage current, and specific changes in trap activation energies.⁷

Low-frequency noise (LFN) characterization is known to be a sensitive tool to investigate the device quality and to track the changes in the structures with aging. In particular $1/f$ noise^{8,9} and random telegraph signal (RTS) noise^{10,11} have been found suitable for study of the physical degradation mechanisms and for reliability estimation. Besides electronic devices, LFN has also been found to be a sensitive

indicator of degradation in optoelectronic devices as quantum-well lasers, optocouplers, and detectors.^{12–15}

In this paper, degradation mechanisms due to accelerated stress are studied in GaN-based LEDs. The aging is due to temperature and electrical stress. The IV and LFN characterizations in frequency and time domain are applied. RTS noise in unstressed and aged samples are related to defects in the junction. The $1/f$ noise at medium currents is related to the crystal quality of the quantum-well (QW) junction and at high currents to the contact resistance quality. The physical mechanisms of degradation are discussed and a noise reliability indicator is proposed.

II. DESCRIPTION OF DEVICES AND EXPERIMENTAL METHODS

The investigated structures are blue GaN LEDs grown on a n -SiC substrate. The active structure consists of an epitaxially grown n -GaN layer followed by an InGaN QW and a top Mg-doped p -GaN layer.⁷ A semitransparent thin platinum film of $300 \times 300 \mu\text{m}^2$ size and about 5-nm thickness is used as top contact. A gold bond wire is contacting in the middle of the contact window, where the optical output is coming through. The ratio between the circular bonding area and window area is 7%.

IV characteristics were performed both in reverse and forward bias using a HP 4145 semiconductor parameter analyzer. LFN measurements in frequency domain were per-

^{a)}Author to whom correspondence should be addressed; electronic mail: dionyz.pogany@tuwien.ac.at

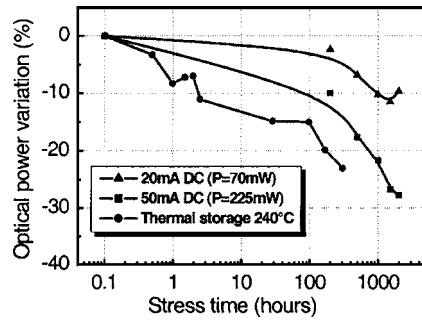


FIG. 1. Optical power degradation as a function of stress duration in GaN LEDs submitted to pure thermal stress and to the dc stress. The connecting lines serve for eye guiding.

formed using a Brookdeal 5004 low-noise voltage preamplifier and an Advantest R9211C spectrum analyzer. Voltage fluctuations (open-circuit voltage noise) were measured in forward-biased diodes using a series resistance with a value of at least ten times higher than the dynamic resistance of the diode. The LFN in time domain was measured using a Keithley 428 current-voltage preamplifier and a digital oscilloscope. RTS fluctuations have been studied in reverse and forward bias.

Two kinds of aging have been performed: an accelerated temperature test (300 h at 240 °C in an oven, denoted by TH) and electrical stress (forward stress currents of $I_{\text{stress}} = 20$ and 50 mA for 2500 h, denoted by S20 and S50, respectively).

Optical measurements were performed using a Newport power meter 1830-C, biasing the device at 20 mA dc. Figure 1 illustrates the output optical power degradation during the three different stresses. The optical power decrease is the strongest for the TH stress and lowest for the S20 stress.

The *IV* and LFN characterizations are performed prior and after aging. LFN noise has been measured at currents up to 20 mA in a Faraday cage. The samples were mounted on a temperature stabilizing heat sink in order to eliminate drift due to temperature fluctuations.

The presented results on unstressed samples (NS), and stressed samples TH, S20, and S50 are typical for sets from one technological lot (two to three samples were studied for a set in a lot). LEDs from three different technology lots have been investigated, showing different series resistances. They exhibit qualitatively similar noise results.

III. ELECTRICAL CHARACTERIZATION RESULTS

A. *IV* characterization

Figure 2 shows the typical *IV* characteristics of unstressed and stressed samples in forward (a) and reverse (b) bias. The forward *IV* curve [see Fig. 2(a)] of an unstressed diode shows at low current ($I < 1 \mu\text{A}$) a higher value for the ideality factor than at medium currents due to tunneling and recombination at the QW. At $I > 0.3 \text{ mA}$ the effect of the series resistance becomes visible. The aging makes two effects visible in forward bias [see Fig. 2(a)]: (i) increase in recombination current and ideality factor η and (ii) an increase in series resistance r_s (see Table I). The recombination current component increase is the lowest for the TH stress,

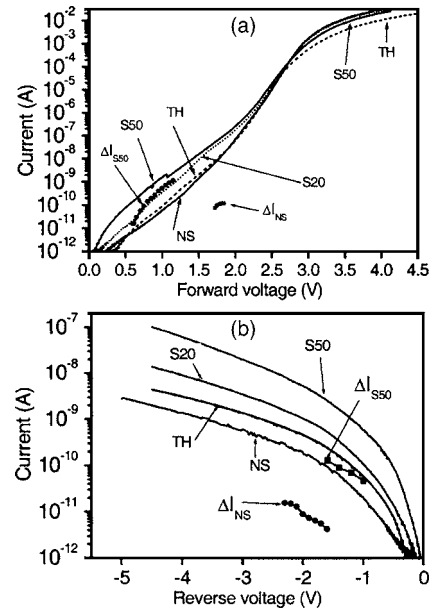


FIG. 2. Forward (a) and reverse (b) bias current-voltage (*IV*) characteristics of as-prepared (NS) and aged (TH, S20, and S50) devices. The *IV* characteristics in (a) and (b) are presented together with typical RTS amplitude-voltage characteristics for unstressed $\Delta I_{\text{NS}}(V)$ and stressed $\Delta I_{\text{S50}}(V)$ devices.

higher for the S20, and is the highest for the S50 stress. The series resistance increase is the highest for TH (90%), medium for S50 (13%), and the lowest for S20 ($\ll 3\%$) devices. For the virgin samples (NS) in the same technological lot, the following spread of current values from sample to sample has been found: In the current region dominated by series resistance, the spread is about 2%. For the intermediate range down to about $0.1 - 1 \mu\text{A}$ the spread is about 10%–20%. The highest spread is observed in the region below 10 nA where the current from sample to sample can vary up to one order of magnitude.

The reverse leakage current [see Fig. 2(b)] of the NS exhibits a strong increase with bias, indicating a defect-assisted tunneling mechanism in the space-charge region.^{11,16} The aging causes an increase in the leakage current with a highest enhancement for the S50, lower for the S20, and lowest for the TH aging.

B. Low-frequency noise characterization

1. $1/f$ noise

Power spectra of voltage fluctuations $S_{V,\text{meas}}$ at two different forward currents I are shown in Fig. 3. The spectrum for $I > 1 \mu\text{A}$ has a $1/f$ spectral shape in the range $1 \text{ Hz} < f < 1 \text{ kHz}$. Such a spectral shape is typical for both unstressed and stressed samples (see curve at $I = 639 \mu\text{A}$). For $I < 1 \mu\text{A}$, the spectrum very often contains a Lorentzian spectrum component on top of the $1/f$ noise due to RTS noise or due to generation-recombination noise (see curve at $I = 0.9 \mu\text{A}$ in Fig. 3). For $I < 20 \text{ nA}$ we often observe the two-level behavior in time domain. The critical current I_{RTS} below which RTS becomes dominant over the $1/f$ in the noise spectrum will be discussed in Sec. IV B.

The measured $1/f$ voltage noise $S_{V,\text{meas}}$ vs I at $f = 1 \text{ Hz}$ for $I > 1 \mu\text{A}$ is given in Fig. 4(a) for unstressed and stressed

TABLE I. Summary of studied samples with measured parameters.

Sample	Aging type	Series resistance r_s	Forward/reverse current	$1/f$ noise, α , and $C_{1/f}$ values	Remark
NS	No	23 Ω	Ideality factor $\eta=3.9$ at 1.5 V	$\alpha=3 \times 10^{-3}$ (at 10 μA) $C_{1/f}=9.4 \times 10^{-12}$ (at 14 mA)	
S20	20 mA/2500 h at room temperature	Typically 23 Ω , increase $\leq 3\%$	Medium increase in forward/reverse current $\eta=5.6$ at 1.5 V	No series resistance noise increase, $C_{1/f}=4 \times 10^{-12}$	Medium increase in defect density in junction/negligible degradation in contact resistance
S50	50 mA/2500 h at room temperature	26 Ω , increase 13%	Largest increase in forward/reverse current $\eta=7.2$ at 1.5 V	50 \times increase in relative series resistance noise, $C_{1/f}=4.4 \times 10^{-10}$, (absolute noise increase $S_{V,\text{meas}}(\text{S50})/S_{V,\text{meas}}(\text{NS})=60 \times$ at 1 Hz)	Largest increase in defect density in junction/medium degradation in contact resistance
TH	Thermal stress 300 h at 240 $^\circ\text{C}$	43 Ω , increase 90%	Lowest increase in forward/reverse current $\eta=6.4$ at 1.5 V	250 \times increase in relative series resistance noise, $C_{1/f}=2.3 \times 10^{-9}$, (absolute noise increase $S_{V,\text{meas}}(\text{TH})/S_{V,\text{meas}}(\text{NS})=800 \times$ at 1 Hz)	Lowest increase (due to annealing) in defect centers in junction/largest degradation in contact resistance

samples. The current noise $S_{I,\text{meas}}$ vs I , calculated from the voltage noise $S_{V,\text{meas}}$ using $S_{I,\text{meas}}=S_{V,\text{meas}}/r_{d,\text{meas}}^2$, is given in Fig. 4(b); the $r_{d,\text{meas}}$ is the experimentally obtained differential resistance of the LED. The following dependences are observed in Fig. 4: (i) $S_{V,\text{meas}} \propto I^{-1}$ for $I < I_c$, and $S_{V,\text{meas}} \propto I^2$ for $I > I_c$ and (ii) $S_{I,\text{meas}} \propto I$ for $I < I_c$ with a leveling off in a transition region and with $S_{I,\text{meas}} \propto I^m$ for $I > I_c$, with $2 < m < 4$. The transition current I_c from the $S_{I,\text{meas}} \propto I$ to $S_{I,\text{meas}} \propto I^m$ ($m \approx 3$) dependence corresponds to the minimum in the $S_{V,\text{meas}}(I)$ characteristics and depends on the degree of stress. The dependence $S_{I,\text{meas}} \propto I$ and $S_{I,\text{meas}} \propto I^3$ will be discussed in Sec. IV A.

The highest value for the transition current $I_c=6$ mA is observed in NS [see Fig. 4(b)]. The S20 sample exhibits no significant change in the noise spectrum compared to the NS. The TH and S50 agings result in a lowering of I_c . For $I > I_c$ a strong $1/f$ noise increase is observed in the S50 ($\approx 60 \times$, $I_c=3$ mA) and in the TH ($\approx 800 \times$, $I_c=0.8$ mA) compared to NS devices. Notice that the spread of noise values from sample to sample in NS for the region $I > I_c$ is only about 20%; therefore, the above result is statistically significant. The $1/f$ noise in all aged diodes for $I < I_c$ only

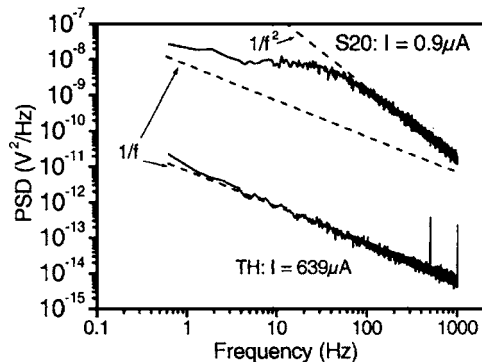


FIG. 3. Power spectral density (PSD) of voltage fluctuations $S_{V,\text{meas}}$ as a function of frequency. A typical pure $1/f$ spectrum for a TH device at constant forward bias current of $I=639 \mu\text{A}$ stems from the junction noise. The noise spectrum at $I=900 \text{ nA}$ for an S20 device shows a Lorentzian contribution due to RTS or g-r noise on top of the $1/f$ noise.

slightly differs from the NS devices [see Figs. 4(a) and 4(b)]. This is a strong indication that TH aging and S50 aging affect more the series resistance than the recombination part of the diode. The three applied stresses leave the junction part of the device relatively unaffected with respect to the $1/f$ noise.

2. RTS in time domain

At forward bias at $I < 20$ nA, two-level or multilevel fluctuations are observed as is shown in the inset of Fig. 5.

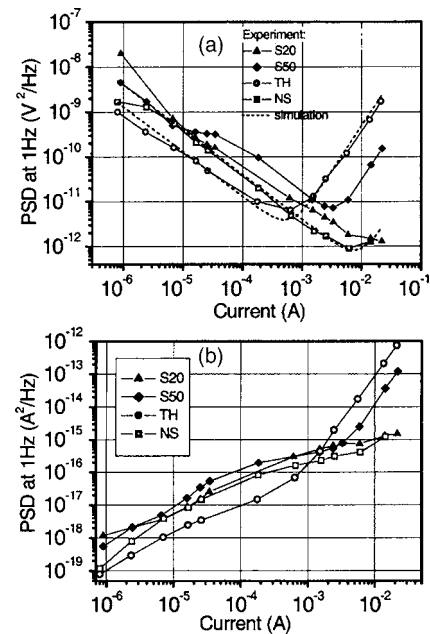


FIG. 4. The power spectral density of the measured voltage noise $S_{V,\text{meas}}$ (a) and calculated current noise $S_{I,\text{meas}}$ (b) at $f=1$ Hz vs the applied forward current for NS, TH, S20, and S50 devices. Two regimes are visible: (i) $S_{V,\text{meas}} \propto I^{-1}$ in (a) which corresponds to $S_{I,\text{meas}} \propto I$ in (b), showing the dominant contribution of the junction noise and (ii) $S_{V,\text{meas}} \propto I^2$ in (a) which corresponds to $S_{I,\text{meas}} \propto I^3$ in (b), showing the dominant contribution of the series resistance noise. The calculated gray lines in (a) are the fitting based on (1a) with $\alpha=3 \times 10^{-3}$, $\tau=10^{-9}$ s, and $r_s=23 \Omega$. The values of $C_{1/f}=9.4 \times 10^{-12}$ and $C_{1/f}=2.3 \times 10^{-9}$ are taken for the NS and TH samples, respectively.

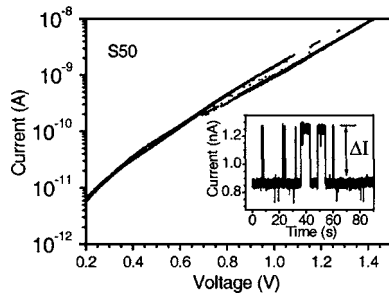


FIG. 5. Slow sweep forward-bias IV curve for an S50 device showing a slow RTS with large relative amplitude. The data are cumulative from ten sweeps. The resolved discrete current levels show that the RTS character is quite stable from one IV run to another. Inset: The corresponding slow RTS fluctuations in time domain at bias $V=0.95$ V; RTS amplitude ΔI is indicated.

Aging causes either (i) creation of new RTS, or (ii) unaffected RTS statistical parameters (i.e., RTS mean pulse widths and amplitude ΔI remain), or (iii) RTS parameter changes, or (iv) vanishing RTS fluctuations.

At forward bias, the relative RTS amplitude $\Delta I/I$ in NS devices is typically less than 5% [see curve ΔI_{NS} in Fig. 2(a)] while in aged devices it can range up to 50% (see curve ΔI_{S50}). Notice a leveling-off tendency in the $\Delta I_{NS}(V)$ curve and a steep increase with current in the $\Delta I_{S50}(V)$ curve at low bias. Both effects can be explained by a strategic position of a RTS-controlling defect in the space-charge region.¹⁷ The slow switching rate of the RTS fluctuations observed in this particular S50 device made it possible to measure individual current levels related to the RTS fluctuations by a IV characterization. Two clear major current branches can be distinguished in Fig. 5. At $V > 1.2$ V the upper branch cannot be observed since the RTS mean pulse width in the upper state decrease with V . A similar effect was observed in forward-biased devices and it was attributed to changes of quasi-Fermi-level relative to the energy position of the controlling RTS trap.^{18,19}

RTS fluctuations distinguishable from Gaussian noise are observed in reverse bias [see Fig. 2(b)]. The dependence $\Delta I(V)$ follows the reverse current–voltage dependence. Similar to forward bias, the maximum value of $\Delta I/I$ in aged samples is higher [$\Delta I/I \approx 10\%$ in curve ΔI_{S50} in Fig. 2(b)] than in NS devices ($\Delta I/I \approx 2\%$ in curve ΔI_{NS}).

IV. DISCUSSION

A. $1/f$ noise spectrum

In this part we discuss the physical origin of the measured $1/f$ noise and separate it into two noise components. The results suggest that the $1/f$ noise in LEDs consists of two components: noise due to the junction part, with $S_I^D \propto I$, dominant in the current region $I < I_C$ and noise from fluctuations in the series resistance r_s , with contribution $S_V = S_r I^2$ dominant in the range $I > I_C$ (see Fig. 4). The $S_{V,meas}(I)$ and $S_{I,meas}(I)$ dependence can be described by the following equation:⁹

$$S_{V,meas} = I^2 S_r + S_I^D r_d^2 \Leftrightarrow S_{I,meas} = \frac{I^2 S_r + S_I^D r_d^2}{r_{d,meas}^2}, \quad (1)$$

where S_r is the spectrum of resistance fluctuations, S_I^D is the current noise in the junction, r_d is the differential resistance of junction, and $r_{d,meas} = r_s + r_d$. The two noise components and the $S_{V,meas}$ and $S_{I,meas}$ dependence on current are discussed below.

1. Junction noise and α value; $S_{I,meas} \propto I$ for $I < I_c$

The $S_I^D \propto I$ part of the $S_{I,meas}(I)$ dependence is attributed to $1/f$ fluctuations in the junction.^{20–23} The $S_{I,meas} \propto I$ dependence has also been observed for the $1/f$ noise in quantum-dot LEDs on InAs–GaAs.¹⁴

Let us calculate the experimental α value (Hooge $1/f$ parameter) from a simple model in order to estimate the quality of the junction. If we assume the diode biased at $I \gg I_0$, where I_0 is the diode saturation current, then the simple charge control approach for current is applicable and simple relations for the $1/f$ noise in the junction can be used. For the current

$$I = \frac{qN}{\tau} \quad (2)$$

holds, where N is the excess carrier number that recombines at the QW in a characteristic time τ . For the $1/f$ noise in the junction (recombination part of a diode)^{20–23}

$$S_I^D = \frac{\alpha q I}{\tau f} \quad (3)$$

holds, with τ in (2) and (3) being the average (radiative) recombination time constant and q the elementary charge. From the experimentally observed current noise below $I_c = 0.8$ mA for the NS, TH, S20, and S50 samples in Fig. 4(b), we observe $S_{I,meas}$ proportional to current as in (3). Using (3) and taking $\tau = 10^{-9}$ s,²⁴ we calculate $\alpha \approx 3 \times 10^{-3}$. This is a figure of merit for the crystal quality of bulk GaN with QW. The α value we found here is in the range of values between 10^{-4} and 10^{-2} often found for GaN in literature^{25–27} and well below the values in the range of 1–150 observed for disordered magnesium-doped p -type GaN grown on sapphire.²⁸

2. Resistance noise; $S_{V,meas} \approx S_r I^2$ for $I > I_C$

In this subsection the origin of exponent $m=3$ in the measured $S_I \propto I^m$ dependence for $I > I_C$ is discussed [see Fig. 4(b)]. The relative $1/f$ noise in the series resistance $C_{1/f}$ is determined from experiments and can be used as a quality parameter.

In the transition region where the series resistance r_s is about the value of the diode junction dynamic resistance r_d we can have the situation that the $1/f$ noise of the series resistance already dominates the contribution of the junction. So for

$$I^2 S_r > S_I^D r_d^2, \quad (4)$$

Eq. (1b) is rewritten as

$$S_{I,\text{meas}} \cong \frac{I^2 S_{r_s}}{(r_d + r_s)^2} = \frac{I^2 S_{r_s} / r_d^2}{(1 + r_s / r_d)^2}. \quad (5)$$

If the series resistance noise is written as

$$S_{r_s} = r_s^2 C_{1/f} / f, \quad (6)$$

where $C_{1/f}$ is the relative $1/f$ noise in the series resistance normalized at 1 Hz, and taking into account $r_d = \eta kT / (qI)$ for $I > I_0$, then we find for the normalized $1/f$ noise at 1 Hz, $fS_{I,\text{meas}}$,

$$fS_{I,\text{meas}} = \frac{C_{1/f} b^2 I^4}{(1 + bI)^2}, \quad (7)$$

where $b = qr_s / (\eta kT)$. The noise ($fS_{I,\text{meas}}$) can be approximated by a power law such as $y = Mx^m$ with $y = fS_{I,\text{meas}}$ and $x = I$, where M is a proportionality factor and m the exponent given by

$$m = \frac{x dy}{y dx} = \frac{4 + 2bI}{1 + bI}. \quad (8)$$

For $m=3$,

$$I = I_c = \eta kT / qr_s, \quad (9)$$

holds. Hence two criteria must be fulfilled to get $m \approx 3$: $I \approx I_c$ (this also means $r_s \approx r_d$) and $C_{1/f} > \alpha q / \tau I_c$ [see (4) and (6)]. This gives for $C_{1/f}$

$$C_{1/f} > \frac{\alpha q^2 r_s}{\tau \eta kT}. \quad (10)$$

The slope $m=3$ has been observed in Fig. 4(b) for the TH and S50 devices under the above conditions for current I_c and $C_{1/f}$. The slope $m=3$ has also been found in a simulation⁹ under the above conditions, $I \geq I_c$, and (10).

The values of $C_{1/f}$ have been extracted from $S_{V,\text{meas}}(I)$ in Fig. 4(a) where $S_{V,\text{meas}} \propto I^2$ holds and the series resistance value has been extracted from the IV characteristics under forward bias. Taking into account (1a) and condition (4), $S_{V,\text{meas}}$ reads

$$S_{V,\text{meas}} = I^2 S_{r_s} + S_I^D r_d^2 \cong I^2 S_{r_s}. \quad (11)$$

For the unstressed devices we calculate from the onset of $S_{V,\text{meas}} \propto I^2$ and taking into account $r_s \cong 23 \Omega$, the lowest value for $C_{1/f} = 9.4 \times 10^{-12}$. The relative series resistance noise is more sensitive for accelerating aging tests than the series resistance value (see Table I). The fitting of experimental curves for the NS and TH samples by (1a) is given in Fig. 4(a).

There is no scientific reason to prefer a presentation of experimental results as open-circuit voltage noise $S_{V,\text{meas}}$ or short-circuit current noise $S_{I,\text{meas}}$. There can only be practical reasons. If the device can be considered as a series connection with independent $1/f$ noise sources in series having different current dependences, then an $S_{V,\text{meas}}$ presentation as function of current is more convenient and easier for interpretation. If the device must be interpreted as a parallel connection of uncorrelated $1/f$ noise sources each with a different current dependency, then an $S_{I,\text{meas}}$ presentation is more appropriate for interpretation.

B. Current criterion $I < I_{\text{RTS}}$ to observe RTS on top of $1/f$ noise

The investigated GaN LEDs show a Lorentzian contribution on top of the $1/f$ noise at low current levels. Here, an upper limit for the current I_{RTS} is derived for observing a possible RTS contribution to the noise spectrum. The calculated results are compared to experiments.

For $I > I_0$ and $I < I_{\text{RTS}}$, we can expect RTS on top of the $1/f$ noise if at least one active trap at the Fermi-level position in the recombination region is present. The $1/f$ noise and RTS noise sources are considered as two independent phenomena as was already proven for GaAs-based quantum-dot light-emitting diodes.¹⁴ Both components of the low-frequency noise were separated and showed a different dependence on current and were uncorrelated. This is a strong indication for a different physical origin for RTS and $1/f$ noise.¹⁴

Machlup²⁹ gives for the RTS noise spectrum

$$\frac{S_{I_{\text{RTS}}}}{I^2} = \frac{S_N}{N^2} = \frac{\overline{(\Delta N)^2}}{N^2} \frac{4\tau_{\text{RTS}}}{1 + (2\pi f \tau_{\text{RTS}})^2}, \quad (12)$$

where S_N is the power spectrum of the carrier number (N) fluctuations and $1/\tau_{\text{RTS}} = 1/\tau_e + 1/\tau_c$ with τ_{RTS} the characteristic time constant of the Lorentzian and τ_e and τ_c the emission and capture time constants, respectively.^{29,30} The maximum value for the variance equals $\overline{(\Delta N)^2} = 1/4$ for $\tau_e = \tau_c$. For a strategic trap located in a high electric field region, we found $\Delta I / I \geq \Delta N / N = 1/N$.³¹ By applying (2) and (12) and replacing ΔN^2 by $K/4$ ($K \geq 1$) we find for symmetric trapping

$$S_{I_{\text{RTS}}} = \frac{Kq^2 \tau_{\text{RTS}}}{\tau^2 [1 + (2\pi f \tau_{\text{RTS}})^2]}, \quad (13)$$

with $K=1$ for a uniform field situation or a trap located at an average electric-field position $E_{\text{loc}} = E_{\text{av}}$, and $K \geq 1$ for traps at strategic high-field locations ($E_{\text{loc}} > E_{\text{av}}$).³¹

$$K = \frac{E_{\text{loc}}^4}{E_{\text{av}}^4}, \quad (14)$$

where E_{loc} is the electric field at the trap location and E_{av} is the average electric field.

Now we compare the $1/f$ noise and the RTS noise at the strategic frequency $f_c = 1/(2\pi\tau_{\text{RTS}})$ because at much lower or higher frequencies than f_c the $1/f$ noise will always be dominant and we are interested in a worst case condition. Then the condition $S_{I_{\text{RTS}}}(f_c) \geq S_I^D(f_c)$ results in

$$\frac{Kq^2 \tau_{\text{RTS}}}{2\tau^2} \geq \frac{2\pi\alpha q I \tau_{\text{RTS}}}{\tau} \quad \text{or} \quad I_{\text{RTS}} \leq \frac{Kq}{4\pi\alpha\tau}. \quad (15)$$

Taking values for an experimentally obtained $\alpha = 3 \times 10^{-3}$ for the GaN structure, assuming $\tau = 10^{-9} \text{ s}$ ²⁴ and taking $K=1$, we expect RTS noise on top of the $1/f$ noise for current $I_{\text{RTS}} < 6 \text{ nA}$. This is consistent with the observations of two-level RTS in Fig. 2(a). One particular experimental result in Fig. 3 has been observed with a Lorentzian at 900 nA: this may stem from a strategic trap at $E_{\text{loc}}/E_{\text{av}} = 3.5$.

C. Aging

Aging degrades junction and series resistance. The physical aspects of the degradation processes will be discussed in the following (see also a brief summary in Table I).

The increase in current and changes in RTS fluctuations after aging indicate creation of new defects and reduction of average nonradiative recombination time constant in the space-charge region. Aging may activate already existing defects, initiating RTS fluctuations. A similar effect was reported in a previous work,³² where it was reported that defect-assisted recombination can cause multiphonon emission with subsequent decrease of the barrier for defect creation. The large relative RTS fluctuation [see $\Delta I/I \approx 50\%$ observed in S50 in Fig. 2(a)] indicates that 50% of current is modulated, possibly by a strategically located trap.^{17–19}

Current increase is lowest for the TH stress (see Fig. 2), while the TH devices exhibit the largest optical power degradation (see Fig. 1) and the largest increase in series resistance noise (see Fig. 4). This suggests that thermal stress mainly affects the contact properties and that defect creation is much lower. The defect creation/enhancement is in fact correlated with the current flow,³² so that the enhancement of defects in thermal stress is lower than that found in current stress (S20 and S50). The slight reduction in junction $1/f$ noise in TH (see Fig. 4) suggests that simultaneously with defect creation, the thermal stress could partially anneal defects in the space-charge region. For the S20 or S50 devices a slight increase of the junction $1/f$ noise is indeed observed in Fig. 4.

The weak variation of the junction noise with electrical aging (see Fig. 4) indicates that the quality of the GaN and QW is only slightly affected by the aging. The decrease of optical output power at certain bias current, after electrical stress (see Fig. 1), can be related to defect-assisted recombination that decrease the injected current into the active region and to the current crowding effect.⁷ The temperature used in the TH stress instead can modify the Mg–H complexes in the p -doped semiconductor region that can strongly decrease the effective doping of the p layer leading to a large increase in the series resistance and contribute to the strong decrease in optical output³³ and also to the increase in the noise.

The strong increase in resistance noise (by a factor of 80–600) together with a weak increase in series resistance value (13%–90%) is a strong indication for the degradation of a part of the series resistance. A very noisy contribution is assumed to be in series with an almost noise-free contribution similar to multispot contact problems.^{9,34–36} The onset of contact degradation leads to current crowding and enhanced noise. The noise of a large part of the series resistance can remain unaffected by the degradation. The above two key conditions⁹ are necessary to have a $C_{1/f} \propto r_s^m$ with $m \gg 5$. This makes noise a much better reliability indicator than r_s itself. Our results support the hypothesis where current crowding was proposed to explain the increase of r_s with aging.^{7,9,34,35}

We assume that the degradation takes place in the semitransparent platinum top layer. This very thin layer (≈ 5 nm) could degrade easily with temperature treatments

and also could be very sensitive to electromigration degradation at high current density. For example, it has been shown that alloying of AuSi contact film on GaAs at temperatures 450 °C and higher causes the formation of globules, thus creating a multispot contact area.³⁶ It is possible that a similar effect could occur in a Pt/GaN contact system. In the S50 device we assume that a local current density of at least 2×10^6 A/cm² must exist at the rim of the semitransparent window and the area around the bonded wire. Such high current densities can provoke electromigration damage around the bonding wire in the thin platinum layer, which is not present in the S20 tests. If the reduction of the real electrical contact area results in a lower current density at the perimeter of the contact window, then the observed decrease in emission at the perimeter⁷ is understood.

V. CONCLUSIONS

Noise characteristics of as-prepared and aged GaN LEDs were investigated. At low currents, an RTS noise on top of $1/f$ noise is observed in forward and reverse bias, due to localized defects in the space-charge region. An expression for a critical current, below which one can expect dominant Lorentzian spectrum from RTS over the $1/f$ noise, has been derived [see Eq. (15)].

At higher forward currents, low-frequency noise consists of two $1/f$ noise components: (i) a junction noise with a dependence $S_{I,\text{meas}} \propto I$ at medium current level and (ii) a series resistance noise with an $S_{V,\text{meas}} \approx S_r I^2$ dependence at higher current levels. The extracted $1/f$ noise parameter $\alpha \approx 3 \times 10^{-3}$ of the junction $1/f$ noise component points to a good crystal quality for the QW region of the LEDs. The relative $1/f$ noise in series resistance normalized at 1 Hz, $C_{1/f}$, is found to be a sensitive diagnostic tool and the conditions for $S_{I,\text{meas}} \propto I^3$ have been derived.

The accelerated aging tests influence the three noise components in a different way. The aging causes a creation/modification of new/already existing RTS noise sources. This is an indication for the creation or electrical activation of localized structural defects in the junction. Because of the random nature of RTS changes with aging, the RTS noise is not a good reliability indicator.

The $1/f$ noise component of the junction is slightly affected by our aging procedures. The junction region quality does not strongly depend on aging. Hence, junction $1/f$ noise is not a very sensitive reliability indicator for this type of aging.

However, at high currents the $1/f$ noise in series resistance strongly depends on degradation by temperature stress (TH) and strong electrical stress (S50). The noise increases as much as a factor of 800, in comparison with a weak increase in series resistance value (factor of 2) after accelerated aging. This typical behavior points to a current crowding effect at the degraded very thin semitransparent platinum contact on top of the p -type GaN layer of the LED. This makes $1/f$ series resistance noise a very sensitive reliability indicator for degradation investigations in GaN LEDs.

ACKNOWLEDGMENTS

The authors would like to thank Dr. Simone Levada (University Padova) and Dr. Jan Kuzmik (TU Vienna and SAS Bratislava) for fruitful discussions. This work was partially supported by the project PRIN 2002 of Italian Ministry of University and Research (MIUR). Professor E. Gornik (TU Vienna) is acknowledged for supporting this work.

- ¹H. Morkoç, *Nitride Semiconductors and Devices* (Springer, Berlin, 1999).
- ²S. Nakamura, S. Senoh, N. Iwasa, and S. Nagahama, *Jpn. J. Appl. Phys.*, Part 2 **34**, L797 (1995).
- ³C.-M. Lee, C.-C. Chuo, Y.-C. Liu, I.-L. Chen, J.-I. Chyi, *IEEE Electron Device Lett.* **25**, 384 (2004).
- ⁴J. Xie and M. Pecht, *IEEE Trans. Device Mater. Reliab.* **3**, 218 (2003).
- ⁵G. Meneghesso *et al.*, *Phys. Status Solidi A* **194**, 389 (2002).
- ⁶G. Meneghesso, A. Chini, A. Maschietto, E. Zanoni, P. Malberti, and M. Ciappa, *Proceedings of the EOS/ESD 2001 Symposium*, Portland, OR 11–13 September 2001 (ESDA, Rome, NY, 2001) p. 249.
- ⁷G. Meneghesso *et al.*, *IEDM'2002*, *IEDM Technical Digest*, San Francisco, CA, 8–11 December 2002 (IEEE, Piscataway, NJ, 2002), p. 103.
- ⁸L. K. J. Vandamme, *IEEE Trans. Electron Devices* **41**, 2176 (1994).
- ⁹L. K. J. Vandamme, *ICNF'2003*, *Proceedings of the 17th International Conference on Noise and Fluctuations*, Prague, Czech Republic, 18–22 August, 2003, edited by J. Sikula (CNRL, Brno, Czech Republic, 2003), p. 735.
- ¹⁰M. J. Deen, S. L. Rumyantsev, and M. Schroter, *J. Appl. Phys.* **85**, 1192 (1999).
- ¹¹D. Pogany, J. A. Chroboczek, and G. Ghibaudo, *J. Appl. Phys.* **89**, 4049 (2001).
- ¹²L. K. J. Vandamme and L. J. van Ruyven, *Proceedings of the Seventh International Conference on Noise in Physical Systems*, Montpellier, France, 17–20 May 1983, edited by M. Savelli, G. Lecoy, and J. P. Nougier (North-Holland, Amsterdam, 1983), p. 245.
- ¹³L. K. J. Vandamme, P. J. L. Herve, and R. Alabedra, *ICNF'1997*, *Proceedings of the 14th International Conference on Noise in Physical Systems*, Leuven, Belgium, 14–18 July 1997, edited by C. Claeys and E. Simoen (World Scientific, Singapore, 1997), p. 495.
- ¹⁴L. K. J. Vandamme, A. V. Belyakov, M. Yu. Perov, and A. V. Yakimov, *Proc. SPIE* **5113**, 368 (2003).
- ¹⁵Y. S. Dai and J. S. Xu, *Solid-State Electron.* **44**, 1495 (2000).
- ¹⁶G. Vincent, A. Chantre, and D. Bois, *J. Appl. Phys.* **50**, 5484 (1979).
- ¹⁷D. Pogany, A. Chantre, J. A. Chroboczek, and G. Ghibaudo, *Appl. Phys. Lett.* **68**, 541 (1996).
- ¹⁸S. T. Hsu, R. J. Whittier, and C. A. Mead, *Solid-State Electron.* **13**, 1055 (1970).
- ¹⁹D. Pogany, S. Ababou, G. Guillot, X. Hugon, B. Vilotitch, and C. Lenoble, *Solid-State Electron.* **38**, 37 (1995).
- ²⁰T. G. M. Kleinpenning, *Physica B & C* **145**, 190 (1987).
- ²¹L. K. J. Vandamme, E. P. Vandamme, and J. J. Dobbela, *Solid-State Electron.* **41**, 901 (1997).
- ²²F. N. Hooge, T. G. M. Kleinpenning, and L. K. J. Vandamme, *Rep. Prog. Phys.* **44**, 479 (1981).
- ²³T. G. M. Kleinpenning, *Physica B & C* **98**, 289 (1980).
- ²⁴M. Kuramoto, Y. Hisanaga, A. Kimura, N. Futagawa, A. A. Yamaguchi, M. Nido, and M. Mizuta, *Semicond. Sci. Technol.* **16**, 770 (2001).
- ²⁵R. Feysaerts, L. K. J. Vandamme, G. Trefan, and M. C. J. C. M. Kramer, *Proceeding of the 31st Solid State Device Research Conference (ESSDERC)*, Nuremberg, Germany, 11–13 September 2001, edited by H. Rysse, G. Wachtka, and H. Grünbacher (Frontier Group, 2001), p. 355.
- ²⁶S. L. Rumyantsev, D. C. Look, M. E. Levinshtein, M. Asif Khan, G. Simin, V. Adivarahan, R. J. Molnar, and M. S. Shur, *Mater. Sci. Forum* **338–342**, 1603 (2000).
- ²⁷S. L. Rumyantsev, M. E. Levinshtein, R. Gaska, M. S. Shur, J. W. Yang, and M. A. Khan, *J. Appl. Phys.* **87**, 1849 (2000).
- ²⁸A. K. Rice and K. M. Malloy, *J. Appl. Phys.* **87**, 7892 (2000).
- ²⁹S. Machlup, *J. Appl. Phys.* **25**, 341 (1954).
- ³⁰M. J. Kirton and M. J. Uren, *Adv. Phys.* **38**, 367 (1989).
- ³¹L. K. J. Vandamme, D. Sodini, and Z. Gingl, *Solid-State Electron.* **42**, 901 (1998).
- ³²S. L. Chuang, A. Ishibashi, S. Kijima, N. Nakayama, M. Ukita, and S. Taniguchi, *IEEE J. Quantum Electron.* **33**, 970 (1997).
- ³³S. M. Myers and A. F. Wright, *J. Appl. Phys.* **90**, 5612 (2001).
- ³⁴R. J. J. M. Jongen, L. K. J. Vandamme, H. H. Bonne, and J. W. C. de Vries, *Fluct. Noise Lett.* **3**, L31 (2003).
- ³⁵L. K. J. Vandamme, M. G. Perichaud, E. Noguera, Y. Danto, and U. Behner, *IEEE Trans. Compon. Packag. Technol.* **22**, 446 (1999).
- ³⁶L. K. J. Vandamme and R. P. Tijburg, *J. Appl. Phys.* **47**, 2056 (1976).